Numerical treatment of long-range Coulomb potential with Berggren bases

N. Michel
Department of Physics, Post Office Box 35 (YFL), University of Jyväskylä, FI-40014 Jyväskylä, Finland

The Schrödinger equation incorporating long-range Coulomb potential takes the form of a Fredholm equation whose kernel is singular on its diagonal when represented by a basis bearing a continuum of states, such as in Fourier-Bessel transform. This phenomenon arises due to the infinite range of Coulomb potential in coordinate space. As a consequence, problems occur when one discretizes the continuum for numerical applications, as the initial kernel becomes a matrix comprising infinite matrix elements. Several methods have been devised to tackle this difficulty, from simply removing infinite-range of Coulomb potential with a screening or cut function to using discretizing schemes which take advantage of the integrable character of Coulomb kernel singularities. However, they have never been tested in the context of Berggren bases, which contains a continuum of complex-energy states and with which both bound and resonant states of complex energy can be expanded. It is the object of this paper to test different discretization schemes of Coulomb potential kernel in the framework of complex-energy physics. Apart from frameworks involving a cut fonction or analytical integration of singularities, a new technique will be presented, which replaces diagonal singularities by finite off-diagonal terms. It will be shown that this methodology surpasses in precision the two former techniques.

I. INTRODUCTION

The infinite-range of Coulomb potential has always been a source of numerous problems in both theoretical and numerical studies of the quantum mechanics of charged particles.

From a theoretical point of view, the $1/r$ Coulomb asymptotics implies the presence of an essential singularity of Coulomb Green's function at $k = 0$ in the complex plane, contrary to that of potentials quickly vanishing at $r \to +\infty$ [1]. This has prevented for a long time from using the simple and elegant demonstration of the completeness of bound and scattering states solutions of the one-body Schrödinger equation of R. Newton [2], as the latter explicitly demands $r^2\ |V(r)|$ to be integrable on $[0 : +\infty[$, where $V(r)$ is the basis-generating potential. Until recently, no simple proof existed for the Coulomb case, as the only available methods requested abstract Lebesgue measure theory [3], thus hindering any physical understanding of this fundamental property. Hence, new methodologies had to be devised in order to have both simple and rigorous demonstrations, based on a generalization of the method of R. Newton [4] or on closeness arguments with standard complete sets of states [5], which heavily rely on the analytical properties of Coulomb wave functions.

At the numerical level, the computational effort necessary to evaluate Coulomb wave functions is tremendous compared to that of its uncharged counterpart, the analytical Ricatti-Bessel function. Indeed, even though analytically expressible in terms of confluent hypergeometric functions [6], Coulomb wave functions are very difficult to calculate, especially in the complex plane [7, 8]. They can vary by many orders of magnitude over a relatively small region and thus demand to employ many different numerical techniques [7, 8]. Added to that, they exhibit a cut in the complex plane on $]-\infty : 0]$, which creates a supplementary difficulty as the functions issued from continued fractions, for example, are analytical therein [7, 8]. When one considers Fourier-Bessel transform of potentials bearing a Coulomb tail, no problem appears at the theoretical level. This comes from the fact that the latter can always be decomposed as $V_0(r)+c/r$, where $V_0(r)$ is a quickly vanishing potential and c is a constant. Indeed, on the one hand, the Fourier-Bessel transform of $V_0(r)$ is well-behaved, and on the other hand, the term proportional to $1/r$ has a Fourier-Bessel transform analytical for all orbital momentum ℓ, equal to $Q_\ell((k^2 + k'^2)/(2kk'))/\pi$, where $Q_\ell(x)$ is the Legendre function of the second kind [6]. However, $Q_\ell(x)$ diverges like $\log(1 - x)$ when $x \to 1$ [9], so that the momentum space representation of $V(r)$ has a logarithmic singularity on its diagonal at $k = k'$, and consequently cannot be discretized readily, as the diagonal of the discretized matrix is infinite. Nevertheless, the Fourier-Bessel transform of $1/r$ is integrable, so that it is possible to solve this problem with subtraction frameworks, where singularities are integrated analytically, leaving a regular rest integral to be handled numerically [10]. This has been successfully applied for the diagonalization of the Coulomb potential in momentum space in Refs.[9, 11, 12].

However, no attempt has been made using Berggren bases [13]. The latter are sets of wave functions generated by finite-range potentials and comprise bound, resonant and scattering states of complex-energy, which are solutions of the one-body Schrödinger equation. Berggren sets of eigenstates are widely used in nuclear physics to solve the many-body problem, as they allow to expand complex nuclear wave functions in a basis of Slater Determinants built from Berggren one-body states, hence within configuration interaction framework (see Ref.[14] for a recent review

on that subject). Due to the presence of scattering states in Berggren bases, the asymptotic behavior of complex many-body wave functions can be precisely reconstructed, which is impossible to attain in practice with bases of well-bound states, such as sets of harmonic oscillator states. They are then very well suited to expand halo and unbound many-body nuclear states [15–25], whose properties cannot be understood without a precise reproduction of their asymptotic properties. Generating potentials are usually of Woods-Saxon type, which mimick the effect of the inert core on valence nucleons [26]. Hartree-Fock potentials are also utilized, as their variational character allows to minimize configuration mixing [19, 22]. In all these cases, wave functions cannot be conveyed in an analytical form and have to be computed numerically. Completeness properties of Berggren sets of states have been established firstly by T. Berggren for uncharged particles [13], while the charged case could be handled only recently in Ref.[5]. Completeness relations have been tested numerically diagonalizing Hamiltonians sustaining spherical and axially-deformed nuclear potentials for both charged and uncharged particles [18, 19, 27, 28], but where Coulomb potential was absent from the diagonalized kernel.

Thus, in this paper, a Hamiltonian possessing an infinite-range proton potential, thus presenting a Coulomb point potential asymptotic, will be diagonalized with Berggren bases employing three different discretization schemes. The first scheme is simply to cut the Coulomb potential at a finite distance R, determined so as to provide optimal results. The second scheme is a subtraction technique, akin to that expressed in Ref.[12], and the third scheme consists in replacing the diverging diagonal elements by off-diagonal terms, which become diagonal at continuum limit. These methods will be described in detail in Sec.(II), where they will be respectively labelled by "the cut method", the "subtraction method" and the "off-diagonal method". Numerical applications will be presented in Sec.(III) for three different partial waves, $s_{1/2}$, $d_{3/2}$ and $d_{5/2}$, where both narrow and broad resonant states will be considered. Numerical methods proper to the use of proton Berggren bases states, generated by a potential with a Coulomb asymptotic, will also be discussed. Conclusion will then be stated in Sec.(IV).

II. THEORETICAL BACKGROUND

A. Expression of the Hamiltonian kernel in a Berggren basis

One considers a Berggren basis of a partial wave of quantum numbers (ℓ, j), whose completeness relation reads [13]:

$$\sum_{n\in(b,d)} u_n(r)u_n(r') + \int_{L^+} u_k(r)u_k(r')\ dk = \delta(r-r'), \tag{1}$$

where L^+ is a complex contour of momenta k starting at $k=0$ and ending at $k=+\infty$, representing the scattering part of the Berggren basis constituted by the $|u_k\rangle$ states, and where the discrete sum runs over bound (b) and resonant, or decaying (d) states $|u_n\rangle$, the latter resonant states being situated between the real k-axis and L^+ (see Ref.[18] for details). The energy of the discrete states $|u_n\rangle$ will be denoted as e_n and that of scattering states $|u_k\rangle$ as e_k. Discrete states $|u_n\rangle$ are normalized to one and scattering states $|u_k\rangle$ to Dirac delta [18]. They are generated by a one-body Hamiltonian of the form:

$$h = \frac{\hat{p}^2}{2m} + V_{WS}(r) + V_c(Z_c, r) \tag{2}$$

$$V_{WS}(r) = -V_o f(r) - 4(\vec{\ell}\cdot\vec{s})V_{so}\frac{1}{r}\left|\frac{df}{dr'}\right|_{r'=r}\ ,\ f(r) = \left[1+\exp\left(\frac{r-R_0}{d}\right)\right]^{-1} \tag{3}$$

$$V_c(Z_c, r) = \frac{C_c\ Z_c\ \mathrm{erf}(\alpha r)}{r}, \tag{4}$$

where m is the effective mass of the proton, $V_{WS}(r)$ is a potential of Woods-Saxon type, with its diffuseness d, radius R_0, central and spin-orbit depths V_o and V_{so}, respectively, $\vec{\ell}$ is the orbital momentum operator and $\vec{s}$ the spin operator, and V_c is the Coulomb potential, proportional to an error function, defined with the Coulomb constant C_c, the charge acting on the proton Z_c and a constant α. The radial function entering the Coulomb potential $V_c(Z_c, r)$ is standard and arises from the use of a Gaussian charge density for the closed core [29–31]. For simplicity, the finite-range part of both basis and diagonalized Hamiltonians will be taken to be the same so that they will differ only through their charge Z_c. We will denote the charge of the basis potential as $Z_c^{(b)}$, that of the diagonalized potential $Z_c^{(d)}$, and their difference, which will enter the kernel to diagonalize, will be denominated as $\Delta Z_c = Z_c^{(d)} - Z_c^{(b)}$. The eigenstate $|\phi\rangle$ of the diagonalized Hamiltonian is to be expanded with Eq.(1):

$$|\phi\rangle = \sum_{n\in(b,d)} c_n|u_n\rangle + \int_{L^+} c_k|u_k\rangle\ dk, \tag{5}$$

where the coefficients c_n and c_k have to be determined. Its energy will be designated as E. Using Eqs.(1,2), the Fredholm equations which must be solved to ascertain the c_n and c_k coefficients are readily inferred:

$$\begin{aligned} c_n\ e_n + \sum_{n' \in (b,d)} c_{n'} \langle u_{n'}|V_c(\Delta Z_c, r)|u_n\rangle + \int_{L^+} c_{k'} \langle u_{k'}|V_c(\Delta Z_c, r)|u_n\rangle\ dk' = E\ c_n\ \forall n \in (b,d), \\ c_k\ e_k + \sum_{n' \in (b,d)} c_{n'} \langle u_{n'}|V_c(\Delta Z_c, r)|u_k\rangle + \int_{L^+} c_{k'} \langle u_{k'}|V_c(\Delta Z_c, r)|u_k\rangle\ dk' = E\ c_k\ \forall k \in L^+. \end{aligned} \tag{6}$$

Matrix elements of Eq.(6) have to be calculated using complex scaling [32, 33] due to the unbound character of basis states:

$$\begin{aligned} \langle u_a|V_c(\Delta Z_c, r)|u_b\rangle\ &= \int_0^R u_a(r) V_c(\Delta Z_c, r) u_b(r)\ dr \\ &+ \sum_{\substack{\omega_a = \pm \\ \omega_b = \pm}} e^{i\theta} \int_0^{+\infty} u_a^{\omega_a}(R + xe^{i\theta}) \frac{C_c\ \Delta Z_c}{R + xe^{i\theta}} u_b^{\omega_b}(R + xe^{i\theta})\ dx, \end{aligned} \tag{7}$$

where $|u_a\rangle$ and $|u_b\rangle$ are two Berggren basis states, R is a radius after which complex scaling is effected, sufficiently large to sustain $\mathrm{erf}(\alpha r) \simeq 1$ and $f(r) \simeq 0$ in Eqs.(3,4), $\omega = \pm$ characterizes the asymptotic character of wave functions components, as $u(r) = u^+(r) + u^-(r) = C^+ H_{\ell\eta}^+(kr) + C^- H_{\ell\eta}^-(kr)$ for $r > R$, $C^\pm$ being a constant and $H_{\ell\eta}^\pm(z)$ a Coulomb wave function of orbital momentum ℓ and Sommerfeld parameter η, of outgoing $(+)$ or incoming $(-)$ character, and θ is the rotation angle, which depends on ω_a and ω_b, chosen so that the associated improper integral converges. Coulomb wave functions are implemented using recently developed techniques mixing analytical formulas and direct integration [8]. Complex scaling is also employed to normalize the discrete states $|u_n\rangle$ (see Eq.(1)) [18]. One has to pay attention if $k(R + xe^{i\theta})$ crosses the negative real axis with complex scaling, as $H_{\ell\eta}^\pm(z)$ becomes discontinuous therein. Indeed, Coulomb wave functions bear a cut therein by definition, whereas the wave functions $u^\pm(r)$ are everywhere continuous, as solutions of a differential equation of second order. Crossing cannot occur in practice for resonant states, sustaining sufficiently small width-to-energy ratios, while non-crossing can be enforced for scattering states by taking a L^+ contour sufficiently close to the real k-axis. It is, however, unavoidable for bound states when $\cos(\theta) < 0$. In the latter case, a linear combination of $H_{\ell\eta}^+(kr)$ and $H_{\ell\eta}^-(kr)$, whose coefficients are simple functions of η and k [8], has to be added to the initial wave function $u(r) = u^+(r) = C^+ H_{\ell\eta}^+(kr)$ to suppress discontinuity. As, for bound states, $|H_{\ell\eta}^-(k(R + xe^{i\theta}))| \to 0$ when $x \to +\infty$ with $\cos(\theta) < 0$, this modification does not change asymptotic properties of $u(r)$.

Due to analyticity of $u_a(r)$ and $u_b(r)$ in the complex r-space, the matrix element embedded in Eq.(7) is independent of R and θ, so that it is a genuine definition of operators acting on Berggren basis states. However, as one might expect, Eq.(7) cannot be used for $|u_a\rangle = |u_b\rangle = |u_k\rangle$. Even though improper integrals for which $\omega_a \omega_b = 1$ are always well defined with complex scaling, no rotation angle θ can be found to have improper integrals converged when $\omega_a \omega_b = -1$. This is straightforward to demonstrate using the asymptotical expressions of $u^\pm(z)$ for $|z| \to +\infty$, which reads:

$$u^\pm(z) \sim \exp[\pm i(kz - \eta \log(2kz))], \tag{8}$$

up to an unimportant constant. As a consequence, similarly to the representation of $1/r$ in momentum space, diagonal matrix elements are infinite, i.e. they cannot be regularized with complex scaling, and off-diagonal matrix elements $\langle u_k|V_c(\Delta Z_c, r)|u_{k'}\rangle$ for which $k \neq k'$, where complex scaling is always available, diverge like $\log(k - k')$ when $k' \to k$. Modification of diagonal matrix elements of Eq.(7) is then necessary to discretize Eq.(6).

B. Discretization of Berggren basis

The most efficient method to discretized Eq.(6) is to utilize a Gauss-Legendre quadrature for the L^+ contour of Eq.(1) [10]. In order to obtain a symmetric matrix in the resulting eigenproblem, discretized scattering states are set equal to $\sqrt{w_{k_i}}\ u_{k_i}(r)$, where w_i is the weight associated to the k_i abscissa. The discretized Berggren completeness relation then reads:

$$\sum_{n \in (b,d)} u_n(r) u_n(r') + \sum_{i=0}^{N_{GL}-1} u_{k_i}(r) u_{k_i}(r')\ w_i \simeq \delta(r - r')$$

$$\Leftrightarrow \sum_{i=0}^{N_{res}-1} u_i(r)u_i(r') + \sum_{i=N_{res}}^{N-1} u_{k_{i_s}}(r)u_{k_{i_s}}(r')\ w_{i_s} \simeq \delta(r-r')$$
$$\Leftrightarrow \sum_{i=0}^{N-1} u_i(r)u_i(r') \simeq \delta(r-r'), \tag{9}$$

where N_{res} is the number of bound/resonant states, N_{GL} is the number of Gauss-Legendre points, $N = N_{res} + N_{GL}$ is the total number of basis states, $i_s = i - N_{res}$, notation which we will maintain for the whole paper, and $u_i(r)$ is a bound/resonant state $u_n(r)$ if $i = n \in [0 : N_{res} - 1]$ and the discretized state $\sqrt{w_{i_s}}\ u_{k_{i_s}}(r)$ if $i \in [N_{res} : N - 1]$. The energy of the i-th state will be designated as e_i. The resulting discretized eigenstate implemented from diagonalization of discretized kernel will be naturally denoted as:

$$|\phi\rangle \simeq \sum_{i=0}^{N-1} c_i |u_i\rangle. \tag{10}$$

C. Cut method

This approximation is the crudest, as it simply removes all improper integrals in Eq.(7), which is equivalent to replace $V_c(Z_c, r)$ of Eq.(4) by $V_c(Z_c, r)\ He(R - r)$, where He is the Heaviside function. As a consequence, Eq.(7) becomes:

$$\langle u_a|V_c(\Delta Z_c, r)|u_b\rangle = \int_0^R u_a(r)V_c(\Delta Z_c, r)u_b(r)\ dr \tag{11}$$

This removes all singularities in the Hamiltonian kernel of Eq.(2), but at the price of introducing a cut-dependence on R which has to be assessed. Its discretized eigenproblem is then straightforward to convey utilizing Eq.(10) (see Sec.(II B) for notations):

$$c_i\ e_i + \sum_{i'=0}^{N-1} c_{i'} \langle u_{i'}|V_c(\Delta Z_c, r)|u_i\rangle = E\ c_i\ ,\ 0 \le i < N. \tag{12}$$

D. Subtraction method

This the standard method to treat integrable singularities in Fredholm kernels [10]. The main idea is to separate the kernel integral into two parts, one whose integrand is regular and the other singular but analytically integrable. However, contrary to the situation of Ref.[12], it is necessary to terminate the L^+ contour at finite $k = k_{max}$. Indeed, allowing the L^+ contour to go to $+\infty$ in the k-plane, with Gauss-Laguerre quadrature for example, would demand to consider wave functions of very high linear momenta, consequently tremendously oscillating. The latter would have to be used in radial integrals which have to be implemented numerically, such as the non-analytical kernels of Eq.(6), hence inducing numerical instability. As, in practice, convergence with k_{max} is rather fast, it is preferrable to utilize Gauss-Legendre quadrature on a L^+ contour ending at $k = k_{max}$.

In order to apply the subtraction method, the integral of Eq.(6) involving k and k' is rewritten the following way:

$$\begin{aligned}
&\int_{L^+} c_{k'} \langle u_{k'}|V_c(\Delta Z_c, r)|u_k\rangle\ dk' \\
&= \int_{L^+} \left[\int_0^{+\infty} \left(c_{k'}\ u_{k'}(r)\ V_c(\Delta Z_c, r)\ u_k(r) - c_k\ s_{k'}(r)\ \frac{C_c\ \Delta Z_c}{r}\ s_k(r) \right) dr \right] dk' \\
&+\ c_k \int_{L^+} \left\langle s_{k'} \left| \frac{C_c\ \Delta Z_c}{r} \right| s_k \right\rangle\ dk',
\end{aligned} \tag{13}$$

where $|s_k\rangle$ is a sine function, i.e. $\langle r|s_k\rangle = \sqrt{2/\pi}\sin(kr)$, so that one has just added and subtracted the $\ell = 0$ Fourier-Bessel transform of the Coulomb potential $(C_c\ \Delta Z_c)/r$. The calculation of the radial integrals inside the first k'-integral of the right-hand side of Eq.(13) can always be performed with complex scaling when $k \neq k'$ (see Sec.(II A)). When $k' \sim k$, the consideration of the asymptotics of $u_k^{\pm}(r)$ for $r \to +\infty$ (see Eq.(8)), the fact that

$2\pi C^+C^- = 1$ (arising from Dirac delta normalization of scattering states [18]) and that $c(k') \sim (k'-k)c'(k)$ ($c(k)$ is an analytic function of k) imply that the radial integrals problematic with complex scaling, i.e. those for which $k = k'$ and $\omega_a\omega_b = -1$ (see Sec.(II A) for notations), are convergent in Eq.(13).

The second integral of the right-hand side of Eq.(13) can be evaluated analytically:

$$\begin{aligned}
&\int_{L^+} \left\langle s_{k'} \left| \frac{C_c\ \Delta Z_c}{r} \right| s_k \right\rangle\ dk' \\
&= \frac{C_c\ \Delta Z_c}{\pi} \left[\int_0^k [\log(k+k') - \log(k-k')]\ dk' + \int_k^{k_{max}} [\log(k+k') - \log(k'-k)]\ dk' \right] \\
&= \frac{C_c\ \Delta Z_c}{\pi} \left[(k_{max}+k)\log(k_{max}+k) - (k_{max}-k)\log(k_{max}-k) - 2\log(k) \right], \qquad (14)
\end{aligned}$$

where the fact that the complex linear momentum k belongs to the L^+ contour has been taken into account. The discretization of Eq.(6) can now be effected, which results in a different treatment of diagonal and off-diagonal terms involving scattering states (see Sec.(II B) for notations):

$$\begin{aligned}
&c_i\ e_i + \sum_{i'=0}^{N-1} c_{i'} \langle u_{i'}|V_c(\Delta Z_c, r)|u_i\rangle = E\ c_i\ ,\ 0 \le i < N_{res} \\
&c_i \left[\int_0^{+\infty} \left(u_i(r)^2\ V_c(\Delta Z_c, r) - w_{i_s}\ s_{k_{i_s}}(r)^2\ \frac{C_c\ \Delta Z_c}{r} \right) dr \right] \\
+\ &c_i\ \frac{C_c\ \Delta Z_c}{\pi} \left[(k_{max}+k_{i_s})\log(k_{max}+k_{i_s}) - (k_{max}-k_{i_s})\log(k_{max}-k_{i_s}) - 2\log(k_{i_s}) \right] \\
-\ &c_i\ \frac{C_c\ \Delta Z_c}{\pi} \sum_{i'_s=0}^{i_s-1} w_{i'_s}\ [\log(k_{i_s}+k_{i'_s}) - \log(k_{i'_s}-k_{i_s})] \\
-\ &c_i\ \frac{C_c\ \Delta Z_c}{\pi} \sum_{i'_s=i_s}^{N_{GL}-1} w_{i'_s}\ [\log(k_{i_s}+k_{i'_s}) - \log(k_{i_s}-k_{i'_s})] \\
+\ &\sum_{\substack{i'=0 \\ i'\neq i}}^{N-1} c_{i'} \langle u_{i'}|V_c(\Delta Z_c, r)|u_i\rangle = E\ c_i\ ,\ N_{res} \le i < N. \qquad (15)
\end{aligned}$$

E. The off-diagonal method

The exchange of the diagonal infinite matrix elements by close off-diagonal matrix elements is motivated by the analytical approximation of the integral of $\log|k-k'|$ between $k'=0$ and $k'=k_{max}$ acquired from the trapezoidal rule. For that, one uses two grids of equally space points on $[0:k]$ and $[k:k_{max}]$, of same discretization step Δk (k_{max} is assumed to be an integral multiple of Δk), so that $N = k/\Delta k$ and $M = (k_{max}-k)/\Delta k$ are their respective number of points. Removing the infinite value at $k'=k$ from the sums deduced from the trapezoidal rule, one obtains:

$$\begin{aligned}
&\int_0^{k_{max}} \log|k-k'|\ dk' = \int_0^k \log(k-k')\ dk' + \int_k^{k_{max}} \log(k'-k)\ dk' \\
\to\ &\sum_{i=0}^{N-1} \log(k-i\Delta k)\ \Delta k + \sum_{i=1}^{M} \log(i\Delta k)\ \Delta k - \frac{\Delta k}{2}\log(k) - \frac{\Delta k}{2}\log(k_{max}-k) \\
=\ &[N\log(\Delta k) + \log(N!) + M\log(\Delta k) + \log(M!)]\Delta k - \frac{\Delta k}{2}\log(k) - \frac{\Delta k}{2}\log(k_{max}-k) \\
=\ &(k_{max}-k)\log(k_{max}-k) - (k_{max}-k) + k\log(k) - k - \Delta k \log\left(\frac{\Delta k}{2\pi}\right) + O(\Delta k^2)\ ,\ \Delta k \to 0. \qquad (16)
\end{aligned}$$

If one replaces the infinite value of $\log|k-k'|$ at $k'=k$ by $\log[\Delta k/(2\pi)]$ in the first line of Eq.(16), its end point contribution of the trapezoidal rule of the integrals defined on $[0:k]$ and $[k:k_{max}]$ at $k'=k$ is equal to $(\Delta k/2)\log[\Delta k/(2\pi)]$, so that $\int_0^{k_{max}} \log|k-k'|\ dk'$ is reproduced up to Δk^2 with the trapezoidal rule, as $\Delta k \log[\Delta k/(2\pi)]$ is then added

to Eq.(16). As a consequence, we introduce the transformation $k \to k - \Delta k/(4\pi)$ and $k' \to k + \Delta k/(4\pi)$ at $k = k'$. This has the advantage not to spoil the precision of the integral if one adds a function $f(k,k')$ regular at $k = k'$ to $\log|k - k'|$, as $f(k - \Delta k/(4\pi), k + \Delta k/(4\pi)) = f(k,k) + O(\Delta k^2)$, immediate from the second-order Taylor expansion of $f(k,k')$ at $k = k'$. Note that $O(\Delta k^2)$ is the error one expects from standard trapezoidal rule.

Even though one cannot assess analytically the error made using Gauss-Legendre quadrature instead of trapezoidal rule, it will be proved to be very small numerically. For that, we consider the following integral:

$$I(k, k_{max}) = \int_0^{k_{max}} \langle s_{k'}|V_c(\Delta Z_c, r)|s_k\rangle \; dk', \tag{17}$$

which is the integral entering Eq.(6) possessing the same singularities as that of Eq.(16), where basis functions $u_k(r)$ have been replaced by sine functions $s_k(r)$ and the complex L^+ contour is hereby the real segment $[0 : k_{max}]$. If one takes $V_c(\Delta Z_c, r)$ to be exactly equal to the point Coulomb potential $(C_c\ \Delta Z_c)/r$, i.e. $\alpha \to +\infty$ in Eq.(4), Eq.(17) is analytical (see Eq.(14)). When α is finite, it is nevertheless possible to evaluate almost exactly the integral of Eq.(17) rewriting $V_c(\Delta Z_c, r)$ as $[V_c(\Delta Z_c, r) - (C_c\ \Delta Z_c)/r] + (C_c\ \Delta Z_c)/r$:

$$\begin{aligned}\int_0^{k_{max}} \langle s_{k'}|V_c(\Delta Z_c, r)|s_k\rangle \; dk' \;&=\; \int_0^{k_{max}} \left\langle s_{k'} \left| V_c(\Delta Z_c, r) - \frac{C_c\ \Delta Z_c}{r} \right| s_k \right\rangle \; dk' \\ &+\; \log(k_{max} - k) - (k_{max} - k) + k\log(k) - k. \end{aligned} \tag{18}$$

As we consider three finite α values for $V_c(\Delta Z_c, r)$ (see Eq.(4)), namely $\alpha = 0.25$, 0.45 and 0.65 fm^{-1}, which correspond respectively to a number of nucleons equal to about 70–80, 10–15 and 5–10, calculating the radial integrals involving $[V_c(\Delta Z_c, r) - (C_c\ \Delta Z_c)/r]$ in Eq.(18) with 300 Gauss-Legendre points defined on $[0 : R]$, with $R = 30$ fm, guarantees an almost exact reproduction of their numerical value. The Gauss-Legendre approximation of Eq.(17) then follows from the transformation mentioned above:

$$I_{GL}(N_{GL}, k_{i_s}, k_{max}) = \sum_{\substack{i'_s=0 \\ i'_s \neq i_s}}^{N_{GL}-1} \langle s_{k_{i'_s}}|V_c(\Delta Z_c, r)|s_{k_{i_s}}\rangle \; w_{i'_s} + \langle s_{k^+_{i_s}}|V_c(\Delta Z_c, r)|s_{k^-_{i_s}}\rangle \; w_{i_s} \tag{19}$$

where $0 \leq i_s < N_{GL}$ and $k^\pm_{i_s}$ is defined as:

$$k^\pm_{i_s} = k_{i_s} \pm \frac{w_{i_s}}{4\pi}\ ,\ 0 \leq i_s < N_{GL}. \tag{20}$$

In order to assess the precision of Eq.(19) when compared to Eq.(17), we define the following relative difference:

$$\Delta I(N_{GL}, k_{i_s}, k_{max}) = \left| \frac{I_{GL}(N_{GL}, k_{i_s}, k_{max}) - I(k_{i_s}, k_{max})}{\max|I(k_{i'_s}, k_{max})|_{0 \leq i'_s < N_{GL}}} \right|. \tag{21}$$

$\Delta I(N_{GL}, k_{i_s}, k_{max})$ is plotted for various values of N_{GL} and k_{max} on Fig.(1). One can see that it is very small, of the order of 10^{-6} to 10^{-5} for $N_{GL} = 50$, and decreases by an order of magnitude when N_{GL} is multiplied by a factor of two. Interestingly, the shape of $\Delta I(N_{GL}, k_{i_s}, k_{max})$ remains identical when N_{GL} is modified, with α and k_{max} kept fixed. Precision is comparable or better than that of point-particle Coulomb potential, especially for α =0.45 and 0.65 fm^{-1}, the values of interest for the lightest nuclei, which are the most studied with Berggren basis [17–25]. As N_{GL} rarely exceeds 100 in practical applications and k_{max} is typically of the order of 4 fm^{-1} [25], the integral discretization inspired from Eq.(16) is justified with Gauss-Legendre quadrature.

We can now proceed to the discretization scheme we advocate for the general Berggren basis from a subtraction method similar to that of Eq.(13). The notations used will be identical to those of Eq.(15) and Sec.(II B). We will also use the following definition:

$$u^\pm_i(r) = \sqrt{w_{i_s}}\ u_{k^\pm_{i_s}}(r)\ ,\ N_{res} \leq i < N, \tag{22}$$

where $k^\pm_{i_s}$ is defined in Eq.(20). The subtraction scheme from which we start is the following:

$$\begin{aligned} &\int_{L^+} c_{k'} \langle u_{k'}|V_c(\Delta Z_c, r)|u_k\rangle \; dk' \\ =\; &\int_{L^+} \left[\int_0^{+\infty} \left(c_{k'}\ u_{k'}(r)\ u_k(r) - c_k\ s_{k'}(r)\ s_k(r)\right) V_c(\Delta Z_c, r)\ dr \right] dk' \\ +\; &c_k \int_{L^+} \langle s_{k'}|V_c(\Delta Z_c, r)|s_k\rangle \; dk', \end{aligned} \tag{23}$$

where Coulomb point potential is no longer utilized, contrary to that of Eq.(13). Based on the latter theoretical and numerical arguments, the discretization scheme of Eq.(15) becomes for Eq.(23):

$$\begin{aligned} & c_i\ e_i + \sum_{i'=0}^{N-1} c_{i'} \langle u_{i'}|V_c(\Delta Z_c, r)|u_i\rangle = E\ c_i\ ,\ 0 \le i < N_{res} \\ & c_i\ \left[e_i + \int_0^{+\infty} \left(u_i(r)^2 - w_{i_s}\ s_{k_{i_s}}(r)^2 \right) V_c(\Delta Z_c, r)\ dr \right] \\ + \ & c_i\ w_{i_s}\ \int_0^{+\infty} s_{k^+_{i_s}}(r) V_c(\Delta Z_c, r) s_{k^-_{i_s}}(r)\ dr \\ + \ & \sum_{\substack{i'=0 \\ i' \neq i}}^{N-1} c_{i'} \langle u_{i'}|V_c(\Delta Z_c, r)|u_i\rangle = E\ c_i\ ,\ N_{res} \le i < N. \end{aligned} \tag{24}$$

All off-diagonal matrix elements involving $s_{k_{i_s}}(r)$ and $s_{k'_{i_s}}(r)$ issued from the integrals of the right-hand side of Eq.(23) cancel out. Indeed, $\int_0^{+\infty} (c_{k'}\ u_{k'}(r)\ u_k(r) - c_k\ s_{k'}(r)\ s_k(r))\, V_c(\Delta Z_c, r)\ dr$ can always be rewritten as $c_{k'}\ \langle u_{k'}|V_c(\Delta Z_c, r)|u_k\rangle - c_k\ \langle s_{k'}|V_c(\Delta Z_c, r)|s_k\rangle$, where the two latter matrix elements can be calculated with complex scaling as $k \neq k'$ (see Sec.(II A)). One can verify that replacing $u_i(r)^2$ by $u_i^+(r)u_i^-(r)$ and $s_{k_{i_s}}(r)^2$ by $s_{k^+_{i_s}}(r)s_{k^-_{i_s}}(r)$ (see Eqs.(20,22)) in the radial integral of the second line of Eq.(24) results in an error of the order of $w_{i_s}^3/(4\pi)^2$, which can be neglected. As $k^+_{i_s} \neq k^-_{i_s}$, the cancellation we have noticed to take place for off-diagonal matrix elements now occurs in the modified diagonal radial integral. The off-diagonal discretization scheme then reads:

$$\begin{aligned} & c_i\ e_i + \sum_{i'=0}^{N-1} c_{i'} \langle u_{i'}|V_c(\Delta Z_c, r)|u_i\rangle = E\ c_i\ ,\ 0 \le i < N_{res} \\ & c_i\ \left[e_i + \langle u_i^+|V_c(\Delta Z_c, r)|u_i^-\rangle \right] + \sum_{\substack{i'=0 \\ i' \neq i}}^{N-1} c_{i'} \langle u_{i'}|V_c(\Delta Z_c, r)|u_i\rangle = E\ c_i\ ,\ N_{res} \le i < N. \end{aligned} \tag{25}$$

Note that the k_{max}-dependence of Eq.(15) has disappeared in Eq.(25), so that this scheme can be used in principle when $k_{max} \to +\infty$.

III. NUMERICAL EXAMPLES

We consider now the expansion of three different states with a Berggren basis, namely proton $1s_{1/2}$, $0d_{5/2}$ and $0d_{3/2}$ wave functions. The parameters defining the Woods-Saxon potential $V_{WS}(r)$ and Coulomb potential $V_c(Z_c, r)$ (see Eqs.(3,4)), common for basis and diagonalized Hamiltonians (see Eq.(2)), are $d = 0.65$ fm, $R_0 = 3$ fm, $V_o = 52$ MeV, $V_{so} = 5$ MeV and $\alpha = 3\sqrt{\pi}/(4R_0)$. The latter value for α is chosen in order for $V_c(Z_c, r = 0)$ to sustain the same value as that of the Coulomb potential defined from a uniformly charged-sphere of radius R_0 [25]. Basis and diagonalized Hamiltonians differ through the value of Z_c in Eq.(4), in which $Z_c^{(b)} = 10$ and $Z_c^{(d)} = 8$ (see Sec.(II A) for notations). These parameters are typical of Woods-Saxon potentials mimicking nuclei of $A \sim 20$ nucleons. The energies and widths of proton states of the basis and diagonalized Hamiltonians, calculated with direct integration, are given in Tab.(I). Note that the proton $0s_{1/2}$ state appears in the $s_{1/2}$ Berggren basis, but, as it is well-bound, the proton $0s_{1/2}$ state just bears perturbative modification from basis to diagonalized Hamiltonian, so that it is not interesting to study its case.

When wielding the cut method (see Sec.(II C)), the cut radius R of Eq.(7) will be fixed at $R = 75$ fm for $s_{1/2}$ and $d_{5/2}$ partial waves, and at $R = 35$ fm for $d_{3/2}$ partial wave, which are the values yielding the best precision for the cut method, while the Berggren basis contour (see Eq.(1)) consists of three segments of the complex k-plane, delimited by the four points $k_{min} = 0$ fm^{-1}, $k = 0.25\text{-}0.1i$ fm^{-1} ($s_{1/2}$ and $d_{5/2}$ partial waves) or $k = 0.4\text{-}0.39i$ fm^{-1} ($d_{3/2}$ partial wave), $k = 1$ fm^{-1} and $k_{max} = 4$ fm^{-1}.

The radial contour employed for complex scaling integration in Eq.(7) is defined by fixing $R = 15$ fm and $\theta = -3\pi/4$, $-\pi/4$, $\pi/4$ or $3\pi/4$. Improper integrals of Eq.(7) are indeed guaranteed to converge employing one of these angular values. The Berggren basis contour used in Eq.(1) is very similar to that of the cut method, except that k_{min} is chosen so that $|F_{\ell\eta}(k_{min}R)| + |k_{min}F'_{\ell\eta}(k_{min}R)| = 10^{-5}$. Indeed, it is necessary for k_{min} to be stricly positive,

because, on the one hand, proton scattering states are very close to regular Coulomb wave functions $\sqrt{2/\pi}F_{\ell\eta}(kr)$ when $k \to 0$ [5], very small for moderate values of r, and on the other hand, $H^{\pm}_{\ell\eta}(kr)$ functions enter complex scaling integration in Eq.(7), which bear very large modulus for moderate values of r. As a consequence, very important numerical cancellations occur between the different improper integrals of Eq.(7). Nevertheless, proton scattering states with very small linear momentum play virtually no role in Berggren basis completeness, because of the very smallness of their amplitudes. Hence, proton scattering states become important only when k_{min} become sufficiently large, and the condition above has been shown to mitigate the numerical instability occurring for $k \sim 0$ while yielding precise results.

Comparison of energies and widths of considered proton states provided by diagonalization to those deduced from direct integration are depicted in Tabs.(II,III,IV). Precision of radial wave functions has also been taken into account by calculating the root mean squares of their real and imaginary parts, defined by:

$$rms(\Re[u]) = \sqrt{\frac{\sum_{i=1}^{N}\left(\Re[u(r_i)] - \Re[u_e(r_i)]\right)^2}{N}} \tag{26}$$

$$rms(\Im[u]) = \sqrt{\frac{\sum_{i=1}^{N}\left(\Im[u(r_i)] - \Im[u_e(r_i)]\right)^2}{N}} \tag{27}$$

where N is taken equal to 512, $r_i = i \cdot (R/N)$, for $1 \leq i \leq N$, is a set of uniformly distributed radii of $[0 : R]$, $u(r)$ is the diagonalized wave function, and $u_e(r)$ is the exact wave function, issued from direct integration. Root mean squares are illustrated in Fig.(2) for all studied cases, i.e. the cut method, the subtraction method and the off-diagonal method (see Secs.(II C,II D,II E)). One can see that the cut method produces very poor results, as it does not even reach the precision acquired with the off-diagonal method when the smallest value of the number of Gauss-Legendre scattering states N_{GL} (see Sec.(II B)) is employed. Moreover, for the $0d_{3/2}$ proton state, although a rather good description of energy and width occurs, the reproduction of the wave function is mediocre. Added to that, the choice of the cut radius could only be effected by comparison with exact results, whereas it has been checked that the two other methods are very robust when the L^+ contour parameters are changed. The best reproduction of the considered proton states clearly arises with the off-diagonal method, for energies, widths and wave functions. The subtraction method, while not being completely inaccurate, saturates very quickly to a wrong value for energies, widths and wave functions, when N_{GL} increases. On the contrary, exponential convergence occurs with the off-diagonal method for both real and imaginary parts of the wave function when N_{GL} augments. This is an intriguing phenomenon, as the subtraction scheme of Eq.(15) is based on a exact calculation of the integral exhibiting singularities, leaving a well-defined function to be integrated numerically, whereas that of Eq.(25), which could be expected at best to be comparable to the subtraction method (see Sec.(II D,II E)), surprisingly surpasses the latter by several orders of magnitudes (see Fig.(2)). It can be explained by noticing that the integrand of the first integral of the right-hand side of Eq.(13), constituted by radial integrals converging with complex scaling (see Eq.(7)), while everywhere finite, is not analytic at $k' \sim k$. Indeed, it is equivalent, up to an unimportant constant, to $(k - k')\log(k - k')$, which does not even possess a finite derivative with respect to k' at $k' = k$. This implies that a Gauss-Legendre discretization of this integral will be far less precise than that of analytic functions, which can usually be well approximated by polynomials. On the contrary, the use of $\langle u_i^+|V_c(\Delta Z_c, r)|u_i^-\rangle$ in Eq.(25) effectively replaces in Eq.(6) the fonction of k' $\langle u_{k'}|V_c(\Delta Z_c, r)|u_k\rangle$, singular at $k' = k$, by an analytic function. Gauss-Legendre quadrature then yields fast convergence to the numerical value of the integral *defined* by the off-diagonal method, which happens to be almost equal to the exact singular kernel (see Sec.(II E)).

IV. CONCLUSION

Bases carrying a continuous part, such as Berggren bases, are very interesting as they allow to expand complex many-body wave functions of loosely bound and unbound states, as both proper asymptotic properties and particle inter-correlations via configuration mixing are present therein. However, the use of Berggren bases is accompanied by mathematical difficulties generated by the unbound character of considered one-body states. Indeed, their completeness properties request many more efforts to be proved than for discrete sets of states, to which the whole apparatus of the theory of compact operators can be applied. Furthermore, the very question of their numerical implementation is challenging in the context of charged particles, as Coulomb wave functions have to be calculated for this type of problem. Discretization of Berggren bases is also central in numerical applications, which is conveniently effected with

Gauss quadrature but demands discretization error to be assessed. Handling of infinite-range interactions is therefore problematic with unbound bases, as the representation of the former give rise to operators bearing singularities, which introduce infinities when Berggren bases are discretized.

In the case of Coulomb potential, kernels are singular but integrable, so that frameworks built from subtraction techniques, based on analytical integration of singularities, have been devised in the context of Fourier-Bessel transform. However, they could not be directly applied to Berggren bases, as they rely on the analytical character of the Fourier-Bessel transform of Coulomb point potential. Hence, in this paper, three different discretization schemes have been studied when Coulomb potential is included in the Hamiltonian to diagonalize, i.e. the cut method, where the Coulomb potential is suppressed after a finite radius R, the subtraction method, similar to those utilized with Fourier-Bessel transform, and a new framework, the off-diagonal method, which amounts to substitute diagonal infinite matrix elements by close but finite off-diagonal matrix elements.

Numerical applications have been considered for three different partial waves, with the examples of $1s_{1/2}$, $0d_{5/2}$ and $0d_{3/2}$ resonant proton states, arising typically from studies of nuclei having $A \sim 20$ nucleons. Woods-Saxon potentials carrying different charges have been employed for basis-generating and diagonalized Hamiltonians. While the cut method could be expected to convey poor precision, the off-diagonal method has been demonstrated to outperform the standard subtraction method. This has been explained by the fact that Gauss-Legendre quadrature is applied within the subtraction method to integrate finite but non-analytic functions, whereas only smooth integrands are treated with Gauss-Legendre quadrature within the off-diagonal method. According to the present study, the latter technique should be taken into account seriously when diagonalizing Hamiltonians possessing an infinite-range Coulomb part.

V. ACKNOWLEDGMENTS

This work was supported by the Academy of Finland and University of Jyväskylä within the FIDIPRO programme.

[1] R.G. Newton, *Scattering Theory of Waves and Particles*, 2nd Ed., (Courier Dover, New York, 2002)
[2] R.G. Newton, J. Math. Phys., **1** (1960) 319
[3] N. Dunford and J.T. Schwartz, *Linear operators*, (Wiley Classics Library, New York, 1988)
[4] A.M. Mukhamedzhanov and M. Akin, Eur. Phys. J A, **37** (2008) 185
[5] N. Michel, J. Math. Phys., **49** (2008) 022109
[6] M. Abramowitz, M. Abramowitz and I.A. Stegun, Editors, Handbook of Mathematical Functions, Applied Mathematics Series, National Bureau of Standards (1972)
[7] I.J. Thompson and A.R. Barnett, Comput. Phys. Comm., **36** (1985) 363; J. Comput. Phys., **64** (1986) 490
[8] N. Michel, Comput. Phys. Comm., **176** (2007) 232
[9] K. Maung Maung, D.E. Kahana and J.W. Norbury, Phys. Rev. D, **47** (1993) 1182
[10] W.H. Press, S.A. Teukolsky, W.T. Vetterling and B.P. Flannery, Numerical Recipes in C, Cambridge University Press (1988,1992).
[11] Y.R. Kwon and F. Tabakin, Phys. Rev. C, **18** (1978) 932
[12] J.W. Norbury, K. Maung Maung and D.E. Kahana, Phys. Rev. A, **50** (1994) 2075
[13] T. Berggren, Nucl. Phys. A, **109** (1968) 265
[14] N. Michel, W. Nazarewicz, M. Płoszajczak and T. Vertse, J. Phys. G, **36** (2009) 013101
[15] R.I. Betan, R.J. Liotta, N. Sandulescu and T. Vertse, Phys. Rev. Lett., **89** (2002) 042501
[16] R.I. Betan, R.J. Liotta, N. Sandulescu and T. Vertse, Phys. Rev. C, **67** (2003) 014322
[17] N. Michel, W. Nazarewicz, M. Płoszajczak and K. Bennaceur, Phys. Rev. Lett., **89** (2002) 042502
[18] N. Michel, W. Nazarewicz, M. Płoszajczak and J. Okołowicz, Phys. Rev. C, **67** (2003) 054311
[19] N. Michel, W. Nazarewicz and M. Płoszajczak, Phys. Rev. C, **70** (2004) 064313
[20] G. Hagen, M. Hjorth-Jensen and N. Michel, Phys. Rev. C, **73** (2006) 064307
[21] K. Tsukiyama, M. Hjorth-Jensen and G. Hagen, Phys. Rev. C, **80** (2009) 051301(R)
[22] G. Hagen, T. Papenbrock and M. Hjorth-Jensen, Phys. Rev. Lett., **104** (2010) 182501
[23] N. Michel, W. Nazarewicz and M. Płoszajczak, Phys. Rev. C, **75** (2007) 031301(R)
[24] N. Michel, W. Nazarewicz and M. Płoszajczak, Nucl. Phys. A, **794** (2007) 29
[25] N. Michel, W. Nazarewicz and M. Płoszajczak, Phys. Rev. C, **82** (2010) 044315
[26] R.D. Woods and D.S. Saxon, Phys. Rev, **95** (1954) 577
[27] A.T. Kruppa, N.Michel and W. Nazarewicz, in Proceedings of the International Conference on Nuclear Physics, Large and Small: Microscopic Studies of Collective Phenomena, presented by W. Nazarewicz at Cocoyoc, Morelos, Mexico, April 19-22, 2004 Eds: Bijker, R. et al. New York, AIP (AIP Conference Proceedings **726**) (2004) 7
[28] G. Hagen and J.S. Vaagen, Phys. Rev. C, **73** (2006) 034321

[29] S. Saito, Suppl. Prog. Theor. Phys., **62** (1977) 11
[30] T. Myo, A. Ohnishi and K. Katō, Prog. Theor. Phys., **99** (1998) 801
[31] R. Id Betan, A.T. Kruppa, and T. Vertse, Phys. Rev. C, **78** (2008) 044308
[32] B. Gyarmati and T. Vertse, Nucl. Phys. A, **160** (1971) 523
[33] B. Simon, Phys. Lett. A, **71** (1979) 211

TABLE I: Energies and widths of proton $1s_{1/2}$, $0d_{5/2}$ and $0d_{3/2}$ states for both basis and diagonalized Hamiltonians, determined with direct integration. Energies are given in MeV and widths in keV. The basis states are denoted as "basis" and the diagonalized states as "diag".

	E basis (MeV)	Γ basis (keV)	E diag (MeV)	Γ diag (keV)
$0s_{1/2}$	-24.4219	0	-25.5752	0
$1s_{1/2}$	1.09747	134.623	0.463324	8.96828
$0d_{5/2}$	1.48359	11.9527	0.666208	0.525611
$0d_{3/2}$	5.07435	1353.51	4.3003	1091.3

TABLE II: Energies and widths of proton $1s_{1/2}$ state issued from the diagonalization of the Hamiltonian of Eq.(2) with $Z_c^{(d)} = 8$, expanded from a Berggren basis generated by a Hamiltonian of same structure but bearing $Z_c^{(b)} = 10$ (see Eqs.(3,4) and Sec.(III) for the values of the other Hamiltonian parameters), as a function of the number of scattering states N_{GL} of the L^+ contour of Eq.(1), discretized with Gauss-Legendre quadrature. E designates the energy of the proton state, given in MeV, and Γ the width of the proton state, given in keV, while "exact" refers to results obtained with direct integration. The different discretization methods, i.e. the cut method, the subtraction method and the off-diagonal method (see Secs.(II C,II D,II E)), are denoted respectively as "cut", "sub" and "off-diag".

N_{GL}	E cut (MeV)	Γ cut (keV)	E sub (MeV)	Γ sub (keV)	E off-diag (MeV)	Γ off-diag (keV)
15	0.461875	-11.6596	0.464574	9.19011	0.46396	10.2211
30	0.465707	13.4833	0.463777	8.26812	0.463343	8.97219
45	0.463476	8.71097	0.463709	8.33267	0.463334	8.96171
60	0.463307	8.68396	0.463681	8.36454	0.463329	8.96458
75	0.463227	8.70558	0.463667	8.38006	0.463328	8.96595
90	0.46284	8.88896	0.463659	8.3888	0.463327	8.96669
105	0.462952	8.69106	0.463654	8.39421	0.463326	8.96712
120	0.462949	8.62468	0.46365	8.3978	0.463326	8.9674
exact	0.463324	8.96828	0.463324	8.96828	0.463324	8.96828

TABLE III: Same as Tab.(II), but for the proton $0d_{5/2}$ state.

N_{GL}	E cut (MeV)	Γ cut (keV)	E sub (MeV)	Γ sub (keV)	E off-diag (MeV)	Γ off-diag (keV)
15	0.664431	3.68108	0.666482	0.234635	0.666428	0.174831
30	0.665162	-6.30699	0.666251	0.586056	0.666216	0.525826
45	0.66623	0.502731	0.66624	0.578586	0.666209	0.527655
60	0.666207	0.52976	0.666237	0.573284	0.666209	0.526746
75	0.666209	0.536367	0.666236	0.5705	0.666209	0.526332
90	0.666206	0.484164	0.666235	0.568849	0.666209	0.52611
105	0.666225	0.502034	0.666234	0.567786	0.666209	0.525978
120	0.666226	0.539324	0.666234	0.567058	0.666209	0.525892
exact	0.666208	0.525611	0.666208	0.525611	0.666208	0.525611

TABLE IV: Same as Tab.(II), but for the proton $0d_{3/2}$ state.

N_{GL}	E cut (MeV)	Γ cut (keV)	E sub (MeV)	Γ sub (keV)	E off-diag (MeV)	Γ off-diag (keV)
15	4.29692	1091.1	4.30016	1091.48	4.30017	1091.49
30	4.30301	1082.24	4.3003	1091.29	4.30031	1091.3
45	4.30016	1091.42	4.3003	1091.29	4.3003	1091.3
60	4.30064	1091.92	4.3003	1091.3	4.3003	1091.3
75	4.30072	1092.15	4.3003	1091.3	4.3003	1091.3
90	4.30064	1091.93	4.3003	1091.3	4.3003	1091.3
105	4.30069	1091.41	4.3003	1091.3	4.3003	1091.3
120	4.30053	1091.58	4.3003	1091.3	4.3003	1091.3
exact	4.3003	1091.3	4.3003	1091.3	4.3003	1091.3

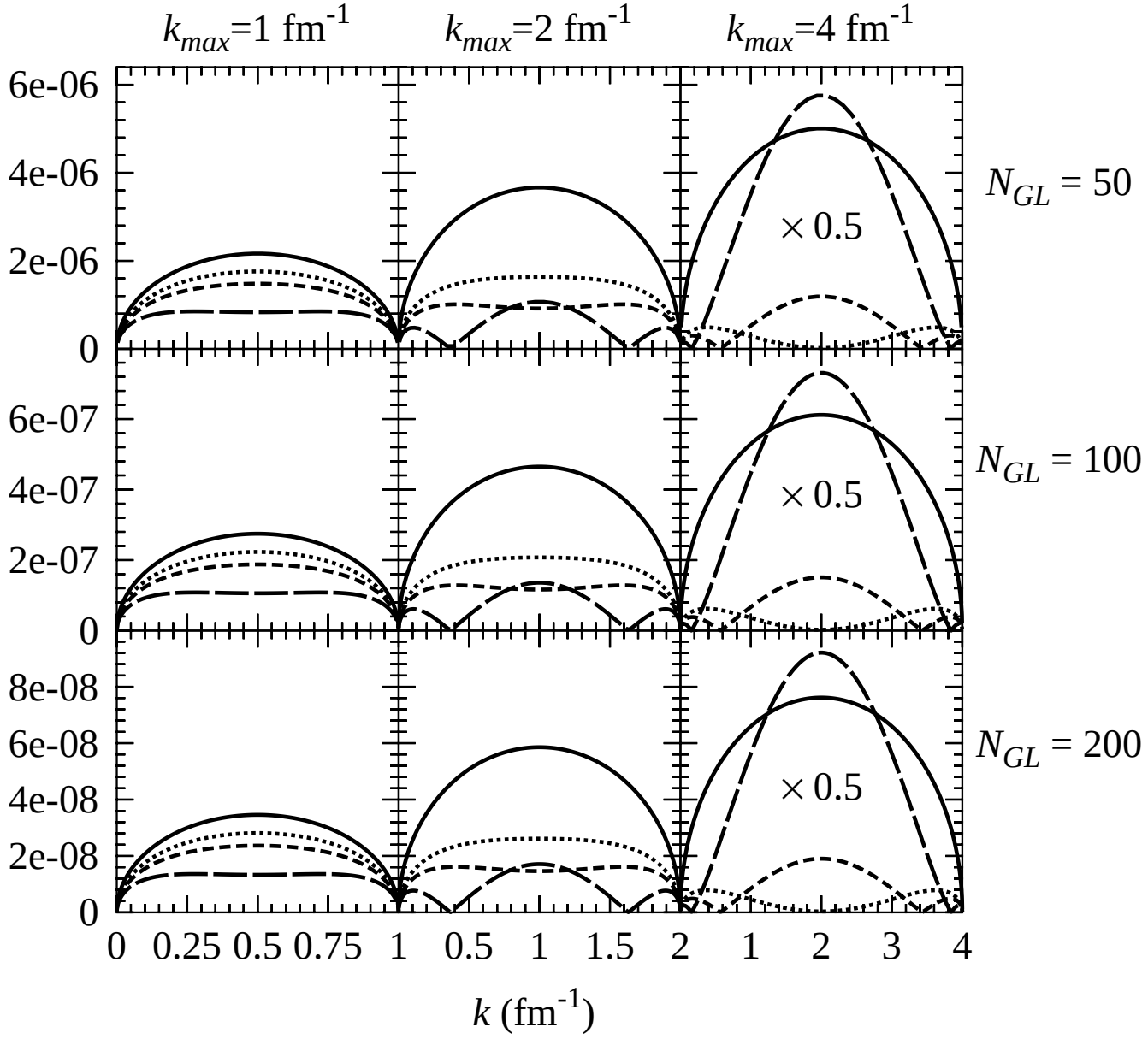

FIG. 1: Relative difference $\Delta I(N_{GL}, k, k_{max})$ (see Eq.(21)) as a function of k. N_{GL} is the number of Gauss-Legendre points in $I_{GL}(N_{GL}, k, k_{max})$ (see Eq.(19)) and k varies from $k = 0$ to $k = k_{max}$. We consider N_{GL} =50, 100 and 200, k_{max} =1, 2 and 4 fm^{-1} and α =0.25, 0.45 and 0.65 fm^{-1}, where α defines the Coulomb potential $V_c(\Delta Z_c, r)$ used (see Eq.(4)). Results are independent of ΔZ_c as it simplifies in $\Delta I(N_{GL}, k, k_{max})$ (see Eq.(21)). Long-dashed, dashed and dotted lines correspond respectively to α =0.25, 0.45 and 0.65 fm^{-1}. Solid lines refer to the use of point-particle Coulomb potential $(C_c\ \Delta Z_c)/r$ instead of $V_c(\Delta Z_c, r)$ in Eqs.(4,17,19). Data corresponding to $k_{max} = 4$ fm^{-1} have been scaled down by a factor of two.

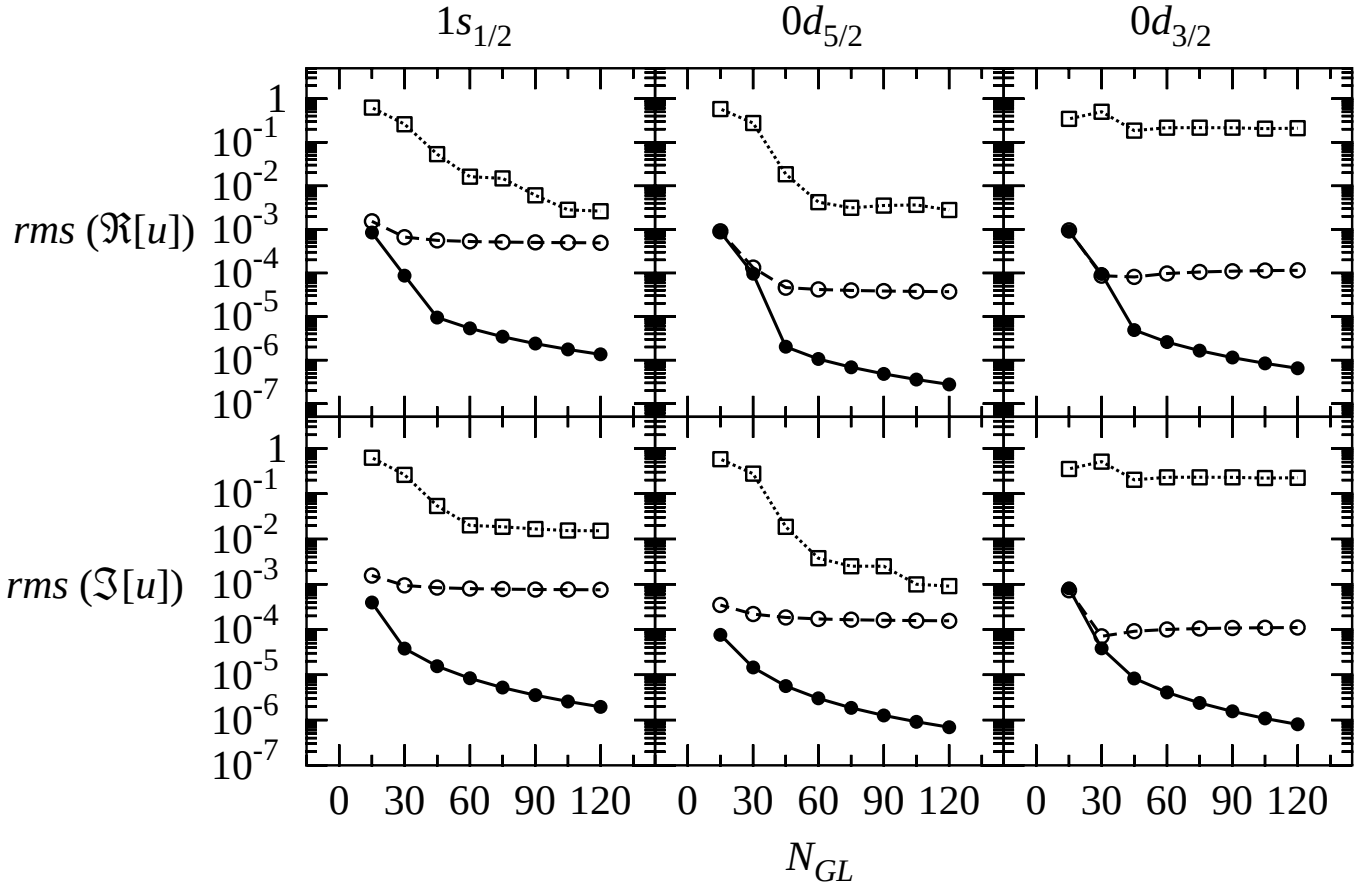

FIG. 2: Root mean squares of the real ($rms(\Re[u])$) and imaginary ($rms(\Im[u])$) parts of diagonalized wave functions $u(r)$ of proton $1s_{1/2}$, $0d_{5/2}$ and $0d_{3/2}$ states (see Eqs.(26,27)), as a function of the number of scattering states discretized with Gauss-Legendre quadrature N_{GL}. Dotted lines with empty squares refer to the cut method (see Sec.(II C)), dashed lines with empty circles to the subtraction method (see Sec.(II D)), and solid lines with filled circles to the off-diagonal method (see Sec.(II E)). Symbols depict the N_{GL} values utilized in calculations while lines guide the eyes.